Investigation of the Atmospheric Oxidation Pathways of Bromoform: Initiation via OH/Cl Reactions

W. Sean McGivern,† Joseph S. Francisco,‡ and Simon W. North*,†

Department of Chemistry, Texas A&M University, 3255 TAMU, College Station, Texas 77842, and Department of Chemistry and Department of Earth and Atmospheric Sciences, Purdue University, West Lafayette, Indiana 47907-1393

Received: February 11, 2002; In Final Form: April 18, 2002

The tropospheric oxidation pathways of bromoform, $CHBr_3$, initiated via reaction with OH and Cl, have been examined computationally with energetics calculated for each mechanistic step up to the liberation of all three bromine atoms. We have calculated the energetics associated with the addition of O_2 to CBr_3 and the subsequent addition of NO to CBr_3O_2 to form an energized peroxy nitrite molecule. The peroxy nitrite molecule is predicted to dissociate rapidly to form CBr_3O and NO_2, and the energetics and kinetics of this step were also determined. We find that the reaction of CBr_3O_2 with HO_2 may directly lead to significant production of CBr_3O, a pathway that is not important in alkyl analogues. We have examined the dissociation of the CBr_3O radical at a higher level of theory to accurately quantify the activation energy and exothermicity of the dissociation. On the basis of our results, we predict that the CBr_3O radical will dissociate rapidly to form Br and CBr_2O. The tropospheric and stratospheric impact of bromoform oxidation is discussed in light of the present results.

I. Introduction

It has been well-established that the role of bromine in stratospheric ozone destruction is significant and is estimated to be approximately equivalent to chlorine as a contributor to the overall destruction of ozone.[1,2] Bromoform, $CHBr_3$, is one of the primary contributors to tropospheric bromine. It is emitted primarily by biogenic marine and photosynthetic processes.[3,4] Bromoform is typically found in significant concentrations in the marine boundary layer where convective transport may provide a mechanism for introduction of bromine into the tropopause, despite its relatively low total atmospheric mixing ratio as compared to methyl bromide and the halons.[5,6] Bromoform has an atmospheric lifetime of ∼2−4 weeks,[7] and recent theoretical models suggest that its degradation contributes more inorganic bromine (Br_y) to the midlatitude lower stratosphere than methyl bromide and the halons combined.[8] Because the degradation of bromoform is important in the formation of the inorganic bromine, an understanding of its tropospheric oxidation mechanism is fundamental in elucidating its overall importance to stratospheric ozone destruction.

The initial steps in the degradation of bromoform in the troposphere involve either oxidation initiated by H-abstraction reactions with OH and Cl or photolysis with lifetimes of 100 days for reaction with OH and ∼35 days for photolysis.[9]

$$CHBr_3 + OH \rightarrow CBr_3 + H_2O$$

$$CHBr_3 + Cl \rightarrow CBr_3 + HCl$$

$$CHBr_3 + h\nu \rightarrow CHBr_2 + Br$$

The rates of reaction with OH and Cl are 1.3×10^{-13} cm^3 s^{-1} (ref 10) and $(3.04 \pm 0.24) \times 10^{-13}$ cm^3 s^{-1} (ref 11), respectively. Although the Cl radical reaction is faster, the OH reaction is expected to dominate overall because of its greater average atmospheric concentration. The oxidation of bromoform is expected to be similar in many aspects to the oxidation of a hydrocarbon.[12] Following abstraction of the hydrogen atom by Cl or OH, the resulting tribromomethyl (CBr_3) radical should react rapidly with O_2 to form the tribromomethyl peroxy radical (CBr_3O_2).

$$CBr_3 + O_2 \rightarrow CBr_3O_2$$

This radical would then be expected to react with NO to form an activated peroxy nitrite molecule, although in a low NO_x environment the reaction with HO_2 may play an important role. The highly excited peroxy nitrite intermediate can then be collisionally stabilized or fragment to form the tribromomethoxy (CBr_3O) radical and NO_2.

$$CBr_3O_2 + NO \rightarrow CBr_3OONO^*$$

$$CBr_3OONO^* \rightarrow CBr_3OONO$$

$$CBr_3OONO^* \rightarrow CBr_3O + NO_2$$

As shown below, the resulting CBr_3O radical would then undergo decomposition to form a free bromine atom and CBr_2O.

$$CBr_3O \rightarrow CBr_2O + Br$$

The reactions of the tribromomethoxy radical have not been examined previously, but in analogy to CCl_3O, the barrier to decomposition is expected to be small and decomposition to be rapid.[13]

In the present study, we have performed ab initio calculations to determine the energetics associated with each step in the

* To whom correspondence should be addressed. Department of Chemistry, Texas A&M University, P.O. Box 30012, College Station, TX 77842. E-mail: north@mail.chem.tamu.ed.

† Texas A&M University.

‡ Purdue University.

10.1021/jp0255886 CCC: $22.00
Published on Web 05/30/2002

oxidation mechanism. We have performed additional calculations at a higher level for the dissociation of the CBr_3O radical and compare the results to previous calculations of the CX_3O (X = H, Cl, F) analogues. In addition, we have modeled the kinetics of the peroxy radical reaction with NO using Rice−Ramsperger−Kassel−Marcus/master equation (RRKM/ME) calculations. Our calculations elucidate the ultimate atmospheric fate of bromoform and provide insight into its contribution to stratospheric bromine concentrations. We also extend the qualitative trends in bromoform oxidation to describe the oxidation of CH_3Br and CH_2Br_2.

II. Calculations

The accurate calculation of bond dissociation energies is difficult, especially for bonds involving elements from the higher rows of the periodic table. Calculations with both large basis sets and high levels of electron correlation are presently beyond the computational capabilities of supercomputers for systems with a large number of bromine atoms. For the present system, we have therefore elected to perform the bond dissociation energy calculations using the coupled cluster with single and double excitations and perturbative triples (CCSD(T)) method with the triple-ζ correlation-consistent polarized valence basis set (cc-pVtz),[14,15,16] which provides an adequate compromise between the treatment of the basis set and correlation effects. Additionally, we have estimated the error due to deviation from the infinite basis set limit for the dissociation of the alkoxy radical by taking the difference in energies calculated at the MP2/cc-pVtz and MP2/cc-pV5z levels. This strategy has previously proven effective at providing an estimate of the correction of the dissociation energies to the infinite basis set limit in haloalkanes.[17] The computational demands of this calculation are severe, and we have not undertaken these calculations for the remaining reactions.

Full geometry optimizations were performed and vibrational frequencies were evaluated using second-order Moller−Plesset perturbation theory (MP2) with full treatment of the core electrons with the 6-311+G* basis set. Transition-state optimizations for $CBr_3O_2^‡$ and $CBr_3O^‡$ were performed at the same level, and frequency calculations were used to confirm their identity. Vibrational frequencies were left unscaled, and all reported energies have been corrected for zero-point energy unless otherwise noted. Calculations were performed using Gaussian 98.[18] MP2 and CCSD(T) calculations for the bond dissociation energies (BDEs) were performed by correlating only the valence electrons (frozen core approximation). A correction of 3.5 kcal/mol was applied to each free bromine atom to account for the known spin−orbit energy of bromine.

III. Results and Discussion

Structures. Optimized geometries were calculated at the MP2(FULL)/6-311+G* level and are shown in Table 1. The ground-state CBr_3O_2 is of C_s symmetry with the O_2 moiety gauche to the carbon−bromine bonds. Transition states for the addition of O_2 were found of the same symmetry in which the O_2 moiety is either eclipsed or gauche to the three carbon−bromine bonds. We find that one of the gauche conformers is lowest in energy and is used in the present calculation of the barrier height. The two BrCBr planes with the common bromine atom opposite the O_2 moiety differ by 146.2° in the CBr_3 reactant molecule, and the planes differ by 139.0° in the CBr_3O_2 transition state. Because the BrCBr planes differ by 125.9° in the CBr_3O_2 product, the transition state appears to occur early in the reaction. An early transition state is expected by the Hammond postulate because of the significant exothermicity of this reaction (Figure 1). The ground-state geometry of the CBr_3O radical was found to be of C_s symmetry, which is consistent with previous studies of the F and Cl analogues by Li and Francisco and may likely be attributed to Jahn−Teller distortion.[13] The ground electronic state of the CBr_3O radical was found to be $^2A'$, and dissociation was assumed to occur along this potential, similar to the case of CF_3O and CCl_3O radicals. The transition state for the loss of bromine from the CBr_3O radical was also found to be of C_s symmetry. The difference in length between the C−Br bonds in the ground-state CBr_3O radical was 0.032 Å. At the transition state, the two bonds lying outside the plane of symmetry have contracted by 0.004 Å, and the bond located in the symmetry plane has stretched by 0.115 Å. The transition state is early, because the Br−C−Br angle (in the remaining radical) increases only slightly at the transition state from 109.81° to 110.45°, despite the planar geometry of the CBr_2O product. The location of the transition state is not unexpected given the exothermicity of the reaction.

TABLE 1: Optimized Geometries for Species Relevant to Bromoform Oxidation[a]

species (symmetry)	coordinate	MP2(FULL)/6-311+G*
CBr_3 (C_{3v})	C−Br	1.873
	∠Br−C−Br	117.0
	∠Br−C−Br−Br	146.2
CBr_3O (C_s)	C−Br	1.952
	C−Br′	1.980
	C−O	1.303
	∠Br−C−Br′	110.9
	∠Br−C−Br	109.8
	∠Br−C−O	113.8
	∠Br′−C−O	97.0
	∠O−C−Br−Br′	108.1
	∠O−C−Br−Br	128.9
$CBr_3O^‡$ (C_s)	C−Br	1.948
	C−Br′	2.095
	C−O	1.246
	∠Br−C−Br′	109.0
	∠Br−C−Br	110.5
	∠Br−C−O	118.0
	∠Br′−C−O	89.7
	∠O−C−Br−Br′	119.7
	∠O−C−Br−Br	140.1
CBr_3O_2 (C_s)	C−Br	1.930
	C−Br′	1.921
	C−O	1.451
	O−O	1.300
	∠Br−C−Br′	111.9
	∠Br−C−Br	111.3
	∠Br−C−O	109.5
	∠Br′−C−O	102.4
	∠O−C−Br−Br′	112.8
	∠O−C−Br−Br	121.3
	∠O−O−C−Br′	180.0
	∠O−O−C−Br	61.2
$CBr_3O_2^‡$ (C_s)	C−Br	1.886
	C−Br′	1.883
	C−O	1.916
	O−O	1.195
	∠Br−C−Br′	115.8
	∠Br−C−Br	114.7
	∠Br−C−O	103.8
	∠Br′−C−O	100.0
	∠O−C−Br−Br′	108.5
	∠O−C−Br−Br	112.5
	∠O−O−C−Br′	180.0
	∠O−O−C−Br	60.1

[a] Distances are given in Å. Angles are given in deg.

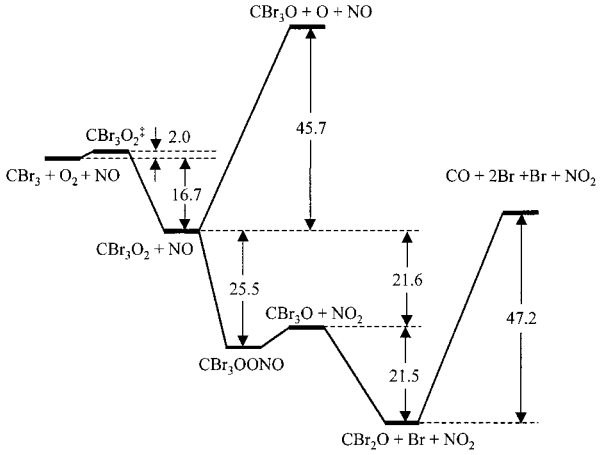

Figure 1. Schematic diagram for the tropospheric oxidation of bromoform. Energies were calculated at the CCSD(T)/cc-pVtz//MP2/6-311+G* level and are zero-point corrected. Energies are given in kcal/mol.

TABLE 2: Calculated Total Energies (hartree) for Species Relevant to Bromoform Oxidation

species	MP2/cc-pVtz	CCSD(T)/cc-pVtz	ZPC (+298 K enthalpy correction)
CBr_3	−7756.017 539 94	−7756.081 046 50	0.005 838 (0.011 816)
CBr_3O	−7831.110 495 64	−7831.189 539 90	0.008 923 (0.016 011)
$CBr_3O^‡$	−7831.109 318 56	−7831.191 182 80	0.008 024 (0.014 845)
CBr_3O_2	−7906.154 425 44	−7906.240 252 50	0.012 794 (0.020 878)
$CBr_3O_2^‡$	−7906.129 256 85	−7906.208 832 80	0.011 205 (0.019 528)
CBr_3OONO	−8035.904 529 23	−8035.996 234 00	0.020 162 (0.029 828)
CBr_2O	−5258.520 345 07	−5258.568 653 10	0.009 318 00 (0.014 604)
Br	−2572.639 452 34	−2572.661 118 60	N/A (0.002 360)
O	−74.954 902 38	−74.973 961 81	N/A (0.002 360)
NO	−129.693 539 68	−129.716 037 79	0.008 036 (0.011 340)
NO_2	−204.779 560 77	−204.800 011 57	0.010 733 (0.014 604)
O_2	−150.110 129 49	−150.128 898 37	0.003 328 (0.006 639)
HO_2	−150.679 604 69	−150.712 006 98	0.014 613 (0.018 409)
CO	−113.135 650 53	−113.155 551 88	0.004 846 (0.008 151)

Comparison to Related Alkoxy Radical Systems. The total energies for each of the species studied in the present work are shown in Table 2, and a schematic diagram illustrating each of the relevant bond dissociation energies and energetic barriers, where applicable, is shown in Figure 1. As shown in the figure, the loss of Br from CBr_3O was found to be exoergic by 21.5 kcal/mol and to occur along a barrierless potential. The C−X bond dissociation energies of the CX_3O halomethoxy radicals formed from a triply halogenated methane derivative are a strong function of the nature of the substituted halogens. Li and Francisco have examined the decomposition pathways of both CF_3O and CCl_3O theoretically.[13] In the case of CF_3O, Li and Francisco reported that the fluorine-loss reaction was strongly endoergic (ΔE = 25.2 kcal/mol) with a barrier of 29.1 kcal/mol, making thermal decomposition unimportant in the troposphere. The cleavage of the C−Cl bond in CCl_3O, however, was found to be strongly exoergic (ΔE = −16.8 kcal/mol) with a small forward barrier (1.3 kcal/mol). The C−O bonds in both species were found to be very strong: 88.6 and 71.7 kcal/mol for CF_3O and CCl_3O, respectively, similar to the C−O bond energy in CBr_3O of 82.5 kcal/mol. Li and Francisco also performed calculations on the mixed F/Cl perhalomethoxy radicals and found that the substitution of fluorine in CCl_3O systematically increased the activation barrier by approximately 2 kcal/mol per fluorine atom.[13] The effect of hydrogen substitution in these species is less clear. Dibble has evaluated the theoretical literature for species of the form $CH_xF_{3-x}O$ and has provided updated values for C−F bond fission in CH_2FO.[19] Though the calculated barrier heights show some variability, they lie in a range of 25.7−31.0 kcal/mol irrespective of the extent of fluorine substitution. We have also performed preliminary calculations on the dependence of the barrier height for Br loss in CH_2BrO and $CHBr_2O$ and find that the dissociation barriers remain unimportant.[20] Although the CH_2ClO and $CHCl_2O$ radicals have not been studied in the same detail, we believe that the qualitative trends in the barrier heights will be approximately constant for each level of halogen subsitution.

Atmospheric Relevance of Bromoform Oxidation. The bromine chemistry of the lower stratosphere has been the subject of recent debate. Initial estimates of the presence of inorganic bromine in the stratosphere suggested that long-lived source gases, such as halons (bromofluorocarbons) and methyl bromide, were the primary contributors to stratospheric bromine. However, more recent studies have indicated that the amount of bromine in the stratosphere is significantly underestimated by models that include only these compounds. Ko et al. have suggested that short-lived source gases, namely, CH_2Br_2 and $CHBr_3$, could contribute significant amounts of bromine to the stratosphere by producing inorganic bromine at a rate faster than its washout rate.[21] Measurements in the tropical tropopause have revealed significant concentrations of bromoform, despite its short atmospheric lifetime compared to methyl bromide.[5] Dvortsov et al. have modeled the transport of bromine-containing compounds to the stratosphere and have found that bromoform is the primary contributor of inorganic bromine to the midlatitude lower stratosphere.[8] More recent modeling studies by Nielsen and Douglass indicate that bromoform represents a lower fraction of stratospheric bromine, though those authors estimate that it contributes approximately one-third of lower stratospheric bromine.[22] The propensity for inorganic bromine formed in the troposphere to be transported to the stratosphere makes the study of bromoform oxidation relevant both to determine the favored products of the reaction and to assist modeling studies in evaluating the stratospheric ozone budget.

Under ambient conditions, the tribromomethyl radical (CBr_3), formed via the abstraction of the hydrogen atom by OH or Cl, will react rapidly with O_2. Typical reaction rates for the addition of O_2 to substituted methylperoxy radicals are on the order of 10^{-12} cm^3 s^{-1}, which implies a lifetime of approximately 1 μs in the lower troposphere and ∼100 μs in the upper atmosphere. Our calculations indicate that O_2 addition to CBr_3 occurs over a small barrier and is exoergic by 16.7 kcal/mol. Transition-state theory (TST) calculations using the ab initio CBr_3O_2 transition-state geometry, frequencies, and energy result in a rate constant on the order of 10^{-17} cm^3 s^{-1}. However, the F and Cl analogues of this system have rate constants on the order of 10^{-12} cm^3 s^{-1}, irrespective of the extent of hydrogen or

halogen substitution.[23] We have therefore performed canonical variational TST calculations using a Morse potential to describe the interaction between the CBr_3 and O_2.[24,25] The calculated rate constant was on the order of 10^{-12} cm^3 s^{-1} using a reasonable treatment of the transitional vibrational modes.[25,26] We therefore predict that the addition of O_2 to CBr_3 occurs along a barrierless potential. The presence of a small barrier at the CCSD(T)/cc-pVtz//MP2/6-311+G* level was also observed in the dissociation of the CBr_3O radical discussed below. After applying a correction to approximate the infinite basis set limit in that species, the energy was found to be less than the asymptotic energy, and we anticipate a similar situation for CBr_3O_2, though these additional calculations were not performed. A photolytic decomposition pathway for the CBr_3 radical is also possible, although we expect it to be unimportant under atmospheric conditions. It is highly unlikely that the CBr_3 radical would have sufficient absorption cross section at wavelengths relevant in the troposphere for this channel to compete with rapid O_2 addition.

The reaction of the resulting tribromomethyl peroxy radical with NO results in an energized peroxy nitrite molecule. We have calculated the energetics associated with the addition of NO to the tribromomethyl peroxy radical to form the peroxy nitrite molecule. The addition step is exoergic by 25.5 kcal/mol, while the subsequent dissociation to form $CBr_3O + NO_2$ is endoergic by only 4.0 kcal/mol because of the weak O−O bond in CBr_3O_2 (vide infra). The energetics are qualitatively similar to other systems in which NO adds to peroxy radicals to form energized peroxy nitrite molecules.[27,28] There is a competition between collisional stabilization of the energized peroxy nitrite molecule and reaction to form an alkoxy radical and NO_2, although for small radicals the latter is expected to dominate.[29] We have performed Rice−Ramsperger−Kassel−Marcus/master-equation (RRKM/ME) calculations[30] to determine the extent of stabilization of the peroxy nitrite molecule. We find that essentially all of the peroxy nitrite molecules decompose rapidly to form vibrationally excited CBr_3O radicals and NO_2 with no stabilization of the CBr_3OONO radicals at atmospherically relevant temperatures and pressures. Though we do not consider direct isomerization to the nitrate molecule in these calculations, previous Fourier transform infrared smog-chamber studies of OH-initiated methyl bromide oxidation found no evidence for either the nitrate or peroxy nitrite molecules.[31]

We have examined the decomposition of the CBr_3O radical at a higher computational level than the remainder of the reaction mechanism. A transition state was located at the MP2/6-311+G* level (full treatment of core electrons). However, a subsequent single-point energy calculation using the correction method described above yielded a total energy lower than that of the reactant, implying that the true transition-state barrier is either very small or that no barrier exists. This reaction is exoergic by 21.5 kcal/mol. This implies the CBr_3O radical will rapidly decompose to form CBr_2O and a free Br atom, likely within a single vibrational period. The average internal energy of the nascent CBr_3O radicals may be determined by applying separate statistical ensembles theory[32] to the results of the RRKM/ME calculations for the CBr_3OONO dissociation channel. We find that on average the CBr_3O radicals have 21 kcal/mol of internal energy. Therefore, the presence of a small barrier on the order of 1 kcal/mol will not significantly affect the overall decomposition mechanism, and dissociation of the CBr_3O radical to form CBr_2O and Br will dominate. In a low-NO_x environment, the resulting CBr_3O radicals will be significantly less energized than when derived from the energized peroxy nitrite molecule based on the energetics of the HO_2 reaction. However, we estimate that, even with a barrier on the order of 1 kcal/mol from a thermal sample, CBr_3O will dissociate prior to a single collision at atmospheric pressures.

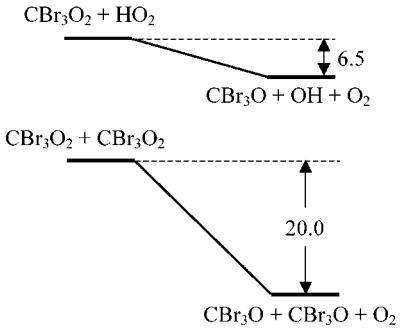

Figure 2. Schematic energy diagrams for the reactions of the tribromomethyl peroxy radical. Energies were calculated at the CCSD(T)/cc-pVtz//MP2/6-311+G* level and are zero-point corrected. Energies are given in kcal/mol.

A schematic diagram for alternative reactions of the tribromomethyl peroxy radical is shown in Figure 2. The reaction of CBr_3O_2 with HO_2 is exoergic by 6.5 kcal/mol with a reaction enthalpy (298 K) of −5.3 kcal/mol. This value is consistent with the decreasing reaction energy of the H, F, and Cl analogues, which have 298 K enthalpies of reaction of +6.5, +4.5, and +0.l kcal/mol, respectively.[23,33] This trend correlates with the strength of the O−O bonds of the CH_3O_2, CF_3O_2, and CCl_3O_2: 59.6, 57.6, and 53.2 kcal/mol, respectively. As shown in Figure 1, the O−O bond energy in CBr_3O_2 is 45.7 kcal/mol. The relative weakness of the O−O bond in CBr_3O_2 with respect to its perhalogenated analogues may allow the reaction of the radical with HO_2 to yield prompt alkoxy radicals. Hydrogen exchange from HO_2 to a peroxy radical results in the formation of a vibrationally excited peroxide species. However, for the perhalogenated peroxy radicals, the endothermicity of the H-, F-, and Cl-containing species ensures that a significant fraction of these radicals will be collisionally stabilized prior to dissociation and can be removed via rainout. The exothermicity of the $CBr_3O_2 + HO_2$ reaction relative to the formation of CBr_3O and OH provides a pathway for the direct formation of CBr_3O even in a low NO_x environment. The CBr_3O will undergo further oxidation to release all three remaining bromine atoms as described below. The importance of this pathway appears to be unique to bromine-containing perhalogenated species, and further examination regarding both halogen and hydrogen substution is clearly warranted. The photolytic decomposition of the CBr_3O radical was also considered. However, the absorption spectrum of this radical is presently unknown, and the role of photolysis in the decomposition of this molecule is unclear, even in areas of low NO_x concentration. We anticipate, however, that the reaction with HO_2 is more important in a low-NO_x environment. We have additionally included the energetics of the self-reaction in Figure 2, which may be important in subsequent laboratory studies of these systems.

The facile C−Br bond cleavage predicted by the ab initio calculations for the alkoxy radicals is consistent with the experimentally observed oxidation products of methyl bromide. Catoire and Niki reported that the loss of Br from the CH_2BrO radical was significantly more important than the reaction with O_2 to form HO_2 and HOCBr, which contributed <10% of the reaction products.[34] Orlando et al. subsequently examined the methyl bromide system and concluded that >95% went to the $CH_2O + Br$ channel.[35] A small amount of HOCBr was observed in the absence of NO, but this reaction was believed to occur

via the peroxy radical self-reaction or reaction of the peroxy radical with HO_2 and was not derived from the alkoxy radical. Orlando et al. assumed a reaction rate for the addition of O_2 and derived an upper limit to the activation energy for Br loss of 7.5 kcal/mol assuming a preexponential factor of 5×10^{14} s^{-1}.[35] Previous work on methyl bromide degradation had assumed that the reaction of the alkoxy radical with O_2 was more important.[36,37] To our knowledge, there is no experimental measurement of the C−Br bond cleavage for CBr_3O. Although the CBr_3O radical would not be expected to react with O_2 because no hydrogen atoms are present, the lack of a barrier in the ab initio calculations provides strong support for a fast decomposition in the CH_2BrO case. The presence of a small barrier, however, would not significantly affect the decomposition rate, because the alkoxy radical formed from the reaction of CBr_3O_2 with NO will be highly vibrationally excited. This behavior differs from the F and Cl analogues of these systems, which have significantly higher barriers to decomposition.[38,39] Lesclaux et al.[38] have studied CCl_3O and found that the decomposition rate was $>1 \times 10^5$ s^{-1} at 223 K, corresponding to an upper limit to the activation energy of 9.6 kcal/mol using the same preexponential factor used by Orlando et al.[35] In addition, the decomposition rate of $CFCl_2O$ was found to be $>3 \times 10^4$ s^{-1} at 253 K corresponding to an activation energy <11 kcal/mol. This trend is also consistent with the ab initio calculations of Li and Francisco on the perhalogenated methoxy radicals, although the calculated barrier heights are lower than these upper limits. Smith et al.[39] examined the CF_2ClO system experimentally and found that the decomposition rate was $>7 \times 10^5$ s^{-1}, which is also consistent with trend.[40]

Following C−Br bond fission in CBr_3O, the fate of CBr_2O involves a competition between photolysis and rainout. We have calculated a C−Br bond dissociation energy in CBr_2O of 47.2 kcal/mol. Recent measurements have established that CBr_2O has an absorption band that extends from 200 to 280 nm.[41] This band covers the first excited state, which is characterized by a $\pi^* \leftarrow n$ transition that results from the nonbonding orbital formed by the orbitals of oxygen and the two bromine atoms and the antibonding orbital from the 2p orbits of the carbon and oxygen.[42] Multireference configuration interaction (MRCI) calculations along the C−Br bond show that dissociation in the first excited state along the C−Br bond proceeds along a repulsive surface. Absorption in the UV band will result in the formation of a bromine atom and BrCO with significant internal energy. However, the BrCO radical is bound by only 0.6 kcal/mol[43] and will release the second bromine atom promptly after loss of the first bromine. Therefore, if CBr_2O photolysis is faster than rainout, the atmospheric oxidation of bromoform under moderate-NO_x conditions should result in the release of all three bromine atoms and oxidation of the carbon to CO.

IV. Conclusions

We have examined numerous steps in the tropospheric oxidation pathway for bromoform using high-level ab initio calculations to evaluate the energetics for each reaction. The addition of O_2 to the CBr_3 radical was found to be strongly exothermic and to occur either over a very small barrier or along a barrierless potential. In a high-NO_x environment, however, NO will add to the CBr_3O_2 radical to form an energized peroxy nitrite molecule, which is expected to rapidly decompose to form vibrationally excited CBr_3O radicals and NO_2. Under low-NO_x conditions, the peroxy radicals likely react with HO_2 to form CBr_3OOH, and O_2. We predict, however, that a nonnegligible fraction of the nascent CBr_3OOH radicals may spontaneously decompose to give CBr_3O and OH. This channel is unimportant in analogous alkyl and haloalkyl systems. The decomposition of the CBr_3O radicals was examined in greater detail by applying a correction to approximate the infinite basis set limit. Though a small barrier was observed at the CCSD(T)/cc-pVtz//MP2/6-311+G* level, the energy at this transition state was found to be lower than that of the products upon application of the correction, and the reaction is expected to occur along a barrierless potential. We therefore anticipate that CBr_3O rapidly decomposes, likely within a vibrational period, to form CBr_2O and Br atoms. Subsequent absorption of a UV photon by CBr_2O will result in the loss of both bromine atoms and oxidation of the carbon to CO.

Acknowledgment. The authors thank Dr. Agnes Derecskei-Kovacs, Dr. Charles E. Webster, and Lisa Thomson for useful comments regarding the ab initio calculations. Jiho Park and Peng Zou are acknowledged for assistance with rate calculations. Hardware and software support from the Texas A&M University Supercomputing Facility and the Texas A&M University Laboratory for Molecular Simulations under the National Science Foundation Grant No. CHE-9528196 is acknowledged. W.S.M. and S.W.N. also acknowledge support from a Texas Research Enhancement Grant. J.S.F. thanks the JPL Supercomputing Project for support of this computing research. The JPL Supercomputing Project is sponsored by JPL and the NASA Office of Space Science and Application.

References and Notes

(1) Rowland, F. S. *Annu. Rev. Phys. Chem.* **1991**, *42*, 731.
(2) Wofsy, S. C.; McElroy, M. B.; Yung, Y. L. *Geophys. Res. Lett.* **1972**, *2*, 215.
(3) Cota, G. F.; Sturges, W. J. *Mar. Chem.* **1997**, *6*, 181.
(4) Class, T.; Kohnle, R.; Ballschmiter, K. *Chemosphere* **1986**, *15*, 429.
(5) Schlauffer, S. M.; Atlas, E. L.; Flocke, F.; Lueb, R. A.; Stroud, V.; Travnicek, W. *Geophys. Res. Lett.* **1998**, *25*, 317.
(6) Sturges, W. T.; Oram, D. E.; Carpenter, L. J.; Penken, S. A. *Geophys. Res. Lett.* **2000**, *27*, 2081.
(7) Barrie, L. A.; Bottenheim, J. W.; Schnell, R. C.; Crutzen, P. J. Rasmussen, R. A. *Science* **1988**, *334*, 138.
(8) Dvortsov, V. L.; Geller, M. A.; Solomon, S.; Schlauffler, S. M.; Atlas, E. L.; Blake, D. R. *Geophys. Res. Lett.* **1999**, *26*, 1699.
(9) Kurylo, M. J.; Rodriguez, M. O.; Andrea, M. O.; Atlas, E. L.; Blake, D. R.; Butler, J. H.; Lal, S.; Lary, D. J.; Midgley, P. M.; Montzka, S. A.; Novelli, P. C., Reeves, C. E.; Simmonds, P. G.; Steele, L. P.; Sturges, W. T.; Weiss, R. T.; Yokouchi, Y. In *Scientific Assessment of Ozone Depletion*; Ennis, C. A., Ed.; World Meteorological Organization: Geneva, Switzerland, 1998; p 2.1.
(10) DeMore, W. B. *J. Phys. Chem.* **1996**, *100*, 5813.
(11) Kambanis, K. G.; Yannis, G. L.; Papagiannakopoulos, P. *J. Phys. Chem. A* **1997**, *101*, 8496.
(12) Finlayson-Pitts, B. J.; Pitts, J. N., Jr. *Chemistry of the Upper and Lower Atmosphere: Theory, Experiments, and Applications*; Academic Press: San Diego, 2000.
(13) Li, Z.; Francisco, J. S. *J. Am. Chem. Soc.* **1989**, *111*, 5660.
(14) Wilson, A. K.; Woon, D. E.; Peterson, K. A.; Dunning, T. H. *J. Chem. Phys* **1999**, *110*, 7667.
(15) Dunning, T. H., Jr. *J. Chem. Phys.* **1989**, *90*, 1007.
(16) Woon, D. E.; Dunning, T. H., Jr. *J. Chem. Phys.* **1993**, *98*, 1358.
(17) McGivern, W. S.; Derecskei-Kovacs, A.; North, S. W.; Francisco, J. S. *J. Phys. Chem. A* **2000**, *104*, 436.
(18) Frisch, M. J.; Trucks, G. W.; Schlegel, H. B.; Scuseria, G. E.; Robb, M. A.; Cheeseman, J. R.; Zakrzewski, V. G.; Montgomery, J. A., Jr.; Stratmann, R. E.; Burant, J. C.; Dapprich, S.; Millam, J. M.; Daniels, A. D.; Kudin, K. N.; Strain, M. C.; Farkas, O.; Tomasi, J.; Barone, V.; Cossi, M.; Cammi, R.; Mennucci, B.; Pomelli, C.; Adamo, C.; Clifford, S.; Ochterski, J.; Petersson, G. A.; Ayala, P. Y.; Cui, Q.; Morokuma, K.; Malick, D. K.; Rabuck, A. D.; Raghavachari, K.; Foresman, J. B.; Cioslowski, J.; Ortiz, J. V.; Stefanov, B. B.; Liu, G.; Liashenko, A.; Piskorz, P.; Komaromi, I.; Gomperts, R.; Martin, R. L.; Fox, D. J.; Keith, T.; Al-Laham, M. A.; Peng, C. Y.; Nanayakkara, A.; Gonzalez, C.; Challacombe, M.; Gill, P. M. W.; Johnson, B. G.; Chen, W.; Wong, M. W.; Andres, J. L.; Head-Gordon, M.; Replogle, E. S.; Pople, J. A. *Gaussian 98*, revision A.6; Gaussian, Inc.: Pittsburgh, PA, 1998.

(19) Dibble, T. S. *J. Mol Struct.* **1999**, *485*−*486*, 67.

(20) Bayes, K.; Friedl, R.; McGivern, W. S.; Kim, H.; Francisco, J. S.; North, S. W., manuscript in preparation.

(21) Ko, M. K. W.; Sze, N.-D.; Scott, C. J.; Weisenstein, D. K. *J. Geophys. Res.* **1997**, *102*, 25507.

(22) Nielsen, J. E.; Douglass, A. R. *J. Geophys. Res.* **2001**, *106*, 8089.

(23) DeMore, W. B.; Sander, S. P.; Howard, C. J.; Ravishankara, A. R.; Golden, D. M.; Kolb, C. E.; Hampson, R. F.; Kurylo, M. J.; Molina, M. J. *Chemical Kinetics and Photochemical Data for Use in Stratospheric Modeling*; JPL Publication 97-4; Jet Propulsion Laboratory: Pasadena, CA, 1997.

(24) McGivern, W. S.; Suh, I.; Clinkenbeard, A. D.; Zhang, R.; North, S. W. *J. Phys. Chem. A* **2000**, *104*, 6609.

(25) The canonical variational transition-state theory calculations used for the present system are described in ref 24. The value of the *a* factor describing the behavior of the transitional vibrational modes is 1.85 $Å^{-1}$.

(26) The change in the rate constant of a factor of 10^5 is due to a combination of the decrease in the barrier height and the use of a loose transition state on a barrierless potential.

(27) Lightfoot, P. D.; Cox, R. A.; Crowley, J. N.; Destriau, M.; Hayman, G. D.; Jenkin, M. E.; Moortgat, G. K.; Zabel, F. *Atmos. Environ. Part A* **1992**, *26*, 1805.

(28) Atkinson, R. *J. Phys. Chem. Ref. Data* **1997**, *26*, 215.

(29) Vereecken, L.; Peeters, J.; Orlando, J. J.; Tyndall, G. S.; Ferronato, C. *J. Phys. Chem. A* **1999**, *103*, 4693.

(30) Park, J.; Zhang, D.; McGivern, W. S.; Zhang, R.; North, S. W., manuscript in preparation.

(31) Sehested, J.; Nielson, O. J.; Wallington, T. J. *Chem. Phys. Lett.* **1993**, *213*, 457.

(32) Wittig, C.; Nadler, I.; Reisler, H.; Noble, M.; Catanzarite, J.; Radhakrishnan, G. *J. Chem. Phys.* **1985**, *83*, 5581.

(33) Sun, H.; Bozzelli, J. W. *J. Phys. Chem. A* **2001**, *105*, 4504.

(34) Catoire, V.; Niki, H. *Chem. Phys. Lett.* **1995**, *245*, 519.

(35) Orlando, J. J.; Tyndall, G. S.; Wallington, T. J. *J. Phys. Chem.* **1996**, *100*, 7026.

(36) Nielsen, O. J.; Munk, J.; Locke, G.; Wallington, T. J. *J. Phys. Chem.* **1991**, *95*, 8714.

(37) Weller, R.; Lorenzenschmidt, H.; Schrems, O. *Ber. Bunsen-Ges. Phys. Chem.* **1992**, *96*, 409.

(38) Lesclaux, R.; Dognon, A. M.; Caralp, F. *J. Photochem. Photobiol., A* **1987**, *41*, 1.

(39) Carr, R. W., Jr.; Peterson, D. G.; Smith, F. K. *J. Phys. Chem.* **1986**, *90*, 607.

(40) Transition-state theory calculations using the parameters from ref 13 yielded preexponential factors of 8×10^{12} and 8.8×10^{12} s^{-1} for Cl loss from CCl_3O and $CFCl_2O$, respectively. These preexponential factors yield activation energies of >8.4 and >9.7 kcal/mol for CCl_3O and $CFCl_2O$ using the measured rates from ref 38.

(41) Hansen, J. C.; Francisco, J. S. Unpublished results.

(42) Li, Y.; Francisco, J. S. *J. Chem. Phys.* **2000**, *113*, 1807.

(43) Dixon, D. A.; Peterson, K. A.; Francisco, J. S. *J. Phys. Chem. A* **2000**, *104*, 6227.